



UNIVERSIDADE ESTADUAL DE CAMPINAS  
SISTEMA DE BIBLIOTECAS DA UNICAMP  
REPOSITÓRIO DA PRODUÇÃO CIENTÍFICA E INTELLECTUAL DA UNICAMP

**Versão do arquivo anexado / Version of attached file:**

Versão do Editor / Published Version

**Mais informações no site da editora / Further information on publisher's website:**

<https://www.sciencedirect.com/science/article/pii/S2666893923000361>

**DOI: <https://doi.org/10.1016/j.carpta.2023.100315>**

**Direitos autorais / Publisher's copyright statement:**

©2023 by Elsevier. All rights reserved.

DIRETORIA DE TRATAMENTO DA INFORMAÇÃO

Cidade Universitária Zeferino Vaz Barão Geraldo

CEP 13083-970 – Campinas SP

Fone: (19) 3521-6493

<http://www.repositorio.unicamp.br>



Contents lists available at ScienceDirect

# Carbohydrate Polymer Technologies and Applications

journal homepage: [www.sciencedirect.com/journal/carbohydrate-polymer-technologies-and-applications](http://www.sciencedirect.com/journal/carbohydrate-polymer-technologies-and-applications)



## Coating of surgical masks with quaternized chitosan aiming at inactivating coronavirus and antibacterial activity

Jonas Kerwald<sup>a</sup>, Celso Fidelis de Moura Junior<sup>a</sup>, Emanuelle Dantas Freitas<sup>a</sup>, Deise Ochi<sup>a</sup>, Rodrigo Sorrechia<sup>b</sup>, Rosemeire Cristina Linhari Rodrigues Pietro<sup>b</sup>, Marisa Masumi Beppu<sup>a,\*</sup>

<sup>a</sup> School of Chemical Engineering, Department of Materials and Bioprocess Engineering, University of Campinas, Av. Albert Einstein, Campinas, São Paulo, 13083-852, Brazil

<sup>b</sup> School of Pharmaceutical Sciences, Department of Drugs and Medicines, São Paulo State University, Rodovia Araraquara-Jaú, Km 1, Araraquara, SP, 14800-903, Brazil

### ARTICLE INFO

#### Keywords:

Coronavirus  
Coating  
Chitosan  
Quaternization  
Inactivation

### ABSTRACT

SARS-CoV-2 caused a global pandemic with high transmission rates, even with widespread vaccination. In addition to isolation and prevention measures, it is important to find new solutions to inactivate the virus and prevent its viability on surfaces, such as clothing and face masks. Chitosan derivatives, with their antibacterial activity, biocompatibility, and non-toxicity, are a promising option for coating these components with virucidal materials. N-(2-hydroxypropyl)-3-trimethylammonium chloride, a quaternized chitosan derivative with degrees of substitution ranging from 59 to 93%, was synthesized. This derivative was used to coat cotton and polypropylene fabrics, such as face masks, without visibly affecting their morphology or filtering capacity. In vitro tests demonstrated that the coatings produced had high antiviral activity against coronavirus, with efficacy up to 99.99%, and were also bactericidal against *E. coli* and *S. aureus*. These results show that quaternized chitosan derivatives have great potential to be used as virucidal coatings, helping to prevent the spread of SARS-Cov-2 and other pathogens on surfaces, which can even be useful for the quick development of solutions for future pandemics.

### 1. Introduction

A series of pneumonia cases were reported throughout December 2019 in Wuhan, China. Early the following month, a new coronavirus (SARS-CoV-2) was isolated, genetically sequenced, and confirmed as the cause of the disease, later named COVID-19. On March 11, 2020, after the global identification of massive infections and deaths in more than 104 countries, the World Health Organization grants the pandemic status to the new coronavirus (Roque-Borda et al., 2023; Gralinski & Menachery, 2020). Despite the development of vaccines capable of decreasing contagion and drastically reducing the severity of symptoms in infected individuals (Katikireddi et al., 2022), several variants of the virus have already been identified and new ones may yet emerge. In addition, although a significant part of the world's population is vaccinated with at least one dose (Mathieu et al., 2021), the emergence of new variants such as omicron (which despite being less deadly, has high transmissibility) due to the stress of basic prevention measures, caused a massive increase in the number of cases worldwide (Das et al., 2022;

Hoffmann et al., 2022). Thus, prevention methods against viral infection remain extremely important.

It is of general interest that techniques and materials capable of inactivating the virus or reducing its viability on surfaces, where it can remain active for up to 9 days, are developed (Kampf et al., 2020). Physical methods of disinfection, such as using steam, UV radiation, or applying high temperatures to a material, are generally preferred over chemical methods because they leave no residue after treatment. The use of virucidal coatings on clothing and face masks could potentially reduce the transmission of SARS-CoV-2 and other infectious agents in high-risk environments, such as hospitals and public transportation, ultimately leading to improved public health outcomes. However, several materials and applications have restrictions regarding temperature and safety, and, in these cases, chemical agents are indicated (Asselt & Giffel, 2005). One strategy for this purpose is to cover personal protective equipment (PPE) with antiviral materials. In this context, quaternary ammonium salts, especially when functionalized on polymers such as chitosan, have already proven to be efficient in inactivating

\* Corresponding author.

E-mail address: [beppu@unicamp.br](mailto:beppu@unicamp.br) (M.M. Beppu).

<https://doi.org/10.1016/j.carpta.2023.100315>

Available online 25 April 2023

2666-8939/© 2023 Published by Elsevier Ltd. This is an open access article under the CC BY-NC-ND license (<http://creativecommons.org/licenses/by-nc-nd/4.0/>).

coronaviruses (Milewska et al., 2013, 2016, 2021).

Chitosan is a biopolymer obtained through the deacetylation of chitin, a compound present in the exoskeleton of crustaceans, arthropods, and some mollusks. Its properties, such as biocompatibility, biodegradability, and antibacterial activity, make the material have several applications in the most diverse fields, mainly in biomedicine (Roque-Borda et al., 2022, 2023). However, its low solubility in water and organic solvents limits its use. To overcome this limitation, chitosan can be modified (Freitas et al., 2020; Qin et al., 2020). Quaternization, for example, which consists of replacing amino terminals of chitosan with quaternary ones, not only improves its solubility but also enhances its antibacterial action, even being reported with antiviral activity against coronaviruses, including SARS-CoV-2.

Chitosan N-(2-hydroxypropyl)-3-trimethylammonium chloride (HTCC), one of the most common chitosan quaternized derivatives, retains many of the characteristic properties of its parent compound, including biocompatibility, mucoadhesiveness, non-toxicity, and antibacterial activity (Freitas et al., 2020; Wang et al., 2020). Studies conducted by Milewska et al. (2013) have shown that HTCC and its derivatives have inhibitory effects on HCoV-NL63. Subsequently, the same group reported that the same compound has virucidal activity against all low-pathogenicity coronaviruses (HCoV-OC43, HCoV-229E, and HCoV-HKU1) (Milewska et al., 2016). Furthermore, subsequent studies have identified HTCC as a potential inhibitor of SARS-CoV-2 and MERS-CoV, coronaviruses of high-pathogenicity (Milewska et al., 2021).

Quaternized chitosan is a promising agent in combating coronaviruses, with potential applications as an adjuvant in vaccines, in the formulation of medicines, or for inactivating the virus on surfaces (J. Zhao et al., 2020). This study aimed at chitosan quaternization to produce HTCC in order to obtain a coating material for surgical masks (either made of cotton or polypropylene). The objective was to effectively inactivate coronavirus and bacteria on these surfaces and significantly reduce their viability.

## 2. Materials and methods

### 2.1. Materials

Chitosan with a degree of deacetylation of 83% and molar mass of 300 kDa, and glycidyltrimethylammonium chloride (GTMAC, >90%) were obtained from Sigma-Aldrich (USA). All the other reagents were used in analytical grade, without any purification step.

The masks, composed of either 100% cotton or 100% polypropylene, were obtained from Real Desc - Máscaras Descartáveis (Brazil). Before going through coating processes, they were functionalized with plasma in an inert atmosphere.

### 2.2. Synthesis of HTCC

The methodology for chitosan quaternization and obtention of HTCC was adapted from the steps performed by Milewska et al. (2016) and Spinelli et al. (2004). In the present study, the reaction was performed in a heterogeneous medium (water). Chitosan of medium molecular weight (83% DD) and GTMAC were used as reactants. 3 g of chitosan were dispersed in 50 mL of milli-Q water for 30 min. Variable volumes of GTMAC (3, 5, or 7 mL) were slowly added to the dispersion. The resultant mixture was kept at 55 °C for 18 h under vigorous stirring in a system with condenser and reflux. The product of the reaction was centrifuged for 20 min. The supernatant was precipitated in a 1:1 (v/v) acetone/ethanol solution for 24 h under stirring. The final purification step was carried out by washing in a Soxhlet Extractor with hot acetone. The resulting white compound was dried at 50 °C for a minimum of 24 h

### 2.3. Characterization of HTCC

#### 2.3.1. Fourier transform infrared spectroscopy (FT-IR)

Fourier-transformed infrared spectra of chitosan and HTCC were obtained on a Nicolet 6700 spectrometer (Thermo Scientific). Samples were prepared with KBr pellets and scanned against a background of blank KBr pellets in the wavelength range 675 to 4000  $\text{cm}^{-1}$  and a scanning rate of 4  $\text{cm}^{-1}$ .

#### 2.3.2. Determination of the degree of substitution of HTCC

The degree of substitution (DS) was determined from conductimetric titration, as reported in the literature (Domard et al., 1986; Li et al., 2015), using a CG2000 bench conductivity meter (Gehaka). The method consists of titration of chlorine ions present in a 0.1 g/dL HTCC solution using a 0.017 M  $\text{AgNO}_3$  solution as a titrator. The reference electrode used was calomel. Thus, the DS of the Examples was calculated according to Eq. (1).

$$DS = \frac{1.7 \times 10^{-5} \times V}{\left[ \frac{W - 1.7 \times 10^{-5} \times V \times MM_{GTMAC}}{MM_G \times DD} + MM_{GA} (1 - D) \right]} \times 100 \quad (1)$$

where V (mL) is the volume of  $\text{AgNO}_3$  used in the titration, W (g) is the mass of HTCC present in solution,  $MM_{GTMAC}$ ,  $MM_G$ , and  $MM_{GA}$  are, respectively, the molecular mass of GTMAC (151 g/mol), of glucosamine (161 g/mol) and acetylated glucosamine (203 g/mol), and DD is the degree of deacetylation of chitosan.

#### 2.3.3. Thermogravimetric analysis (TGA)

The TGA curves of the samples were obtained from a thermal analyzer model DTG-60 (Shimadzu, Japan) at a heating rate of 10 °C/min, under an inert atmosphere of nitrogen and in the range of 25 °C to 700 °C.

#### 2.3.4. Determination of HTCC solubility

The solubility of HTCC samples was estimated through an empirical method based on Cho et al. (2006). According to the authors, HTCC becomes insoluble in water when the transmittance of the compound at 600 nm is lower than 50% of deionized transmittance at the same wavelength. The transmittances were obtained in a Shimadzu 1800 spectrophotometer using HTCC solutions ranging from 0,1 to 5 g/dL. Concentrations over 5 g/dL generate solutions with high viscosity, which are not suitable for this method because the obtained values of transmittance are not reliable and reproducible.

### 2.4. Coating of facemasks with HTCC

HTCC solutions were prepared from 0.1 g of the product added to 100 mL of water, and the system was kept under magnetic stirring for 24 h until the total dissolution of the product. The solutions were placed in sprayers that were used to deposit the material on  $2 \times 2 \text{ cm}^2$  pieces of cotton and polypropylene (PP) fabrics, previously treated with atmospheric plasma to improve adhesion of HTCC in the mask as plasma causes the production of free radicals. The spray jet was applied on each side of the mask at a fixed distance of 20 cm. Finally, the textile substrates were dried in an oven at 50 °C for 1 h

### 2.5. Characterization of coatings

To verify the morphological, topographical, and growth aspects of the films, in addition to obtaining information regarding their surface chemistry, the characterization techniques of characterization mentioned below were used.

#### 2.5.1. FT-IR

The infrared spectra of the HTCC-coated masks were obtained using a Nicolet 6700 spectrometer (Thermo Scientific) with an attenuated

total reflection (ATR) Smart Omni sampler accessory, in the range of 670 to 4000  $\text{cm}^{-1}$  and a scanning rate of 4  $\text{cm}^{-1}$ .

### 2.5.2. Coated masks morphology

The morphology of the different masks coated with HTCC was investigated by scanning electron microscopy (SEM) in Leo 440i SEM equipment (LEO, USA).

### 2.6. Antiviral activity and cytotoxicity assay

L929 cells (ATCC CCL-1) were grown in Dulbecco's Modified Eagle's Medium (DMEM) supplemented with 10% fetal bovine serum (FBS) and 5%  $\text{CO}_2$  at 37 °C in 96-well plate. Next, viral inactivation was assessed by Spearman and Karber's (Ramakrishnan, 2016) endpoint method through serial dilution. In this method, before contact with the L929 cells, the masks covered with HTCC (samples of  $2 \times 2 \text{ cm}^2$ ) were put in contact with MHV-3 strains (viruses of the same genus and family as the SARS-CoV-1 and SARS-CoV-2), at a concentration of  $10^8/\text{mL}$  in 500  $\mu\text{L}$  at room temperature. After the determined contact time, the viral solution was serially diluted, from 10 to  $10^8$ , and transferred to plates containing monolayers of L929 cells. The system was then incubated for 48 h with 5%  $\text{CO}_2$  at 37 °C. The cytopathic and cytotoxic effects of the samples were examined using an inverted optical microscope. As the viral concentration in each dilution is known, the cytopathic effect (cell death) can be obtained by counting dead cells, indicating the sufficient presence of the virus to promote such an effect. The inhibitory effect can then be expressed by the logarithmic reduction of the virus, according to Eq. (2).

$$\text{Log}_{\text{reduction}} = \log_{10} \left( \frac{A}{B} \right) \quad (2)$$

where A is the amount of viable virus before contact with the virucidal material, and B is the amount of viable virus after treatment.

### 2.7. Antibacterial activity assay

#### 2.7.1. Minimum inhibitory concentration (MIC)

The minimum inhibitory concentration tests were carried out to evaluate the HTCC in solution, not being applied to coatings. The bacterial strains (*E. coli* ATCC 25,922 and *S. aureus* ATCC 25,923) were inoculated in agar (Brain-Heart Infusion) and incubated for approximately 18 h at 37 °C. The medium was picked from the plate in Mueller Hinton broth (MH) and incubated again for the same period and temperature. The inoculum concentration was adjusted in 0.9% saline solution until turbidity on the 0.5 McFarland scale ( $1.5 \times 10^8 \text{ CFU/mL}$ ). A 1:1000 dilution was made in MH broth ( $1.5 \times 10^6 \text{ CFU/mL}$ ). 100  $\mu\text{L}$  of MH broth was added to all wells of the 96-well microplate. To the wells of the first column were added 100  $\mu\text{L}$  of the HTCC samples with 3 different degrees of substitution. Ampicillin was used as a control antibiotic. Then, a serial dilution was performed with the transfer of 100  $\mu\text{L}$  from the wells of a column to the subsequent other of the microplate, until reaching the end of the column. 100  $\mu\text{L}$  of inoculum was added to all wells except control wells. Plates for each bacterium were incubated at 37 °C for 24 h

To obtain MBC, samples were collected from each well of the microplate before the addition of resazurin, which were seeded on MH agar using autoclaved wooden rods. The medium was incubated at 37 °C for 24 h. Finally, the concentration corresponding to the last well without microbial growth was defined as MBC.

#### 2.7.2. Diffusion in agar

The assay described in this section was based on CLSI Standard M2-A13. Using the same inoculum prepared in Section 2.7.1, 100  $\mu\text{L}$  of the bacterial suspension was added to the Mueller Hinton plate and spread with a Drigalsky loop in all directions. 20  $\mu\text{L}$  of the control antibiotic

were applied to part of the filter paper discs and tissues. The samples, 4 per plate, were inserted at equidistant points on the plate, pressing lightly with tweezers to favor the diffusion of the samples. They were incubated at 37 °C for 24 h. The diameter of the inhibition halos of each sample, if any, was measured using a caliper.

#### 2.7.3. Colony counting assay

The test was based on JIS L 1902 and ISO 20,743 standards (adapted). *E. coli* ATCC 25,922 and *S. aureus* ATCC 25,923 strains were incubated, with medium adjustment and dilution, analogous to that described in Section 2.7.1. However, the test was performed in 50 mL falcon tubes, with 200  $\mu\text{L}$  of the bacterial suspension poured onto the tissues. The system was incubated for 24 h at 37 °C. 20 mL of saline was added with vortexing. The resulting solution was diluted in ratios of 1:10 and 1:100, which were plated on 100  $\mu\text{L}$  Mueller-Hinton agar, in triplicate, with subsequent incubation for 24 h at 37 °C. Finally, colonies on each plate were counted.

## 3. Results and discussion

### 3.1. Characterization of chitosan

The FTIR spectra of chitosan and HTCC are shown in Fig. 1. Comparing the spectrum of chitosan with that of HTCC, one observes the emergence of a characteristic peak close to 1479  $\text{cm}^{-1}$ . According to Huang et al. (2014), this peak corresponds to the angular deformation of the C–H bond of the trimethylammonium group, confirming its presence in the quaternized sample, replacing the N–H bond present in chitosan at 1590  $\text{cm}^{-1}$  (referring to the angular deformation of the N–H bond of the primary amine). The other characteristic peaks, referring to the polysaccharide structure, pyranose, and O–H bonds, are still present after chitosan quaternization.

The conductimetric titration of HTCC solutions with  $\text{AgNO}_3$  resulted in the curves shown in Fig. 2. While  $\text{AgNO}_3$  is added to HTC the C solution,  $\text{Ag}^+$  ions react with counter ion  $\text{Cl}^-$  from HTCC which leads to a decrease in conductivity until it reaches a minimum value due to  $\text{AgCl}$  salt formation. This minimum value is relative to the moment when all  $\text{Cl}^-$  was consumed, and the amount of  $\text{AgNO}_3$  added was used to determine DS (Table 1). The addition of more  $\text{AgNO}_3$  from this point on elevates the conductivity due to the excess of  $\text{Ag}^+$ . An increase in the DS demonstrates that a higher amount of GTMAC increases the concentration of substituent groups. The amount of GTMAC solution used

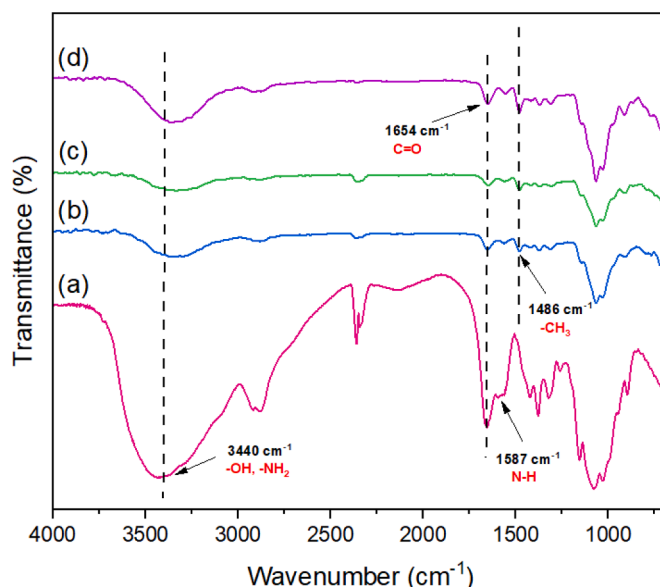


Fig. 1. FTIR spectra of chitosan (a), HTCC\_3 (b), HTCC\_5 (c) and HTCC\_7 (d).

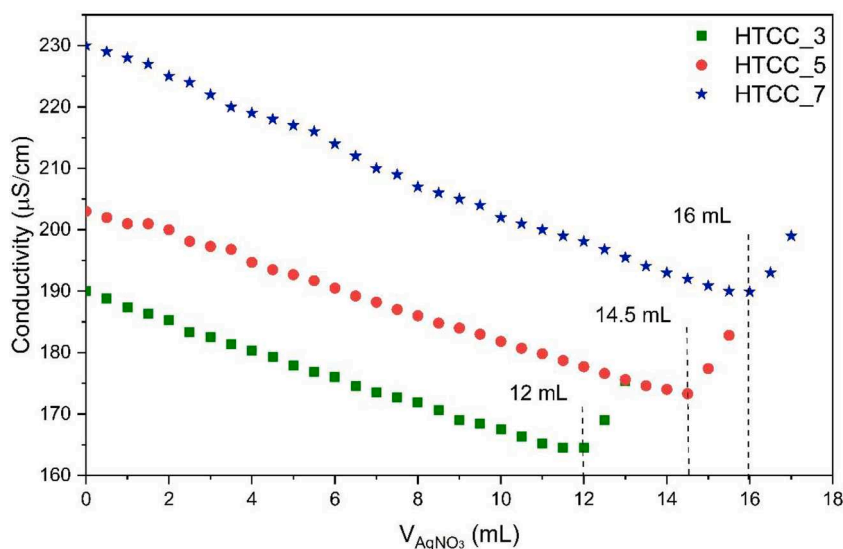


Fig. 2. Conductometric titration of different HTCC samples.

Table 1

Degree of substitution and solubility of HTCC samples.

HTCC_n	$V_{AgNO_3}$ (mL)	DS (%)	Solubility (g/dL)
HTCC_3	12	59	11.8
HTCC_5	14.5	79	16.7
HTCC_7	16	93	22.6

during the execution of the methodology took experimental aspects into consideration. Volumes of GTMAC that were smaller than 3 mL did not displace the reaction sufficiently to produce an adequate amount of HTCC for characterization. In conditions above 7 mL of GTMAC in the reaction medium, it was not possible to properly agitate due to a sharp increase in the viscosity of the medium. Thus, the minimum and maximum values (3 and 7 mL) of the GTMAC solution represent an optimal range that favors the heterogeneous reaction.

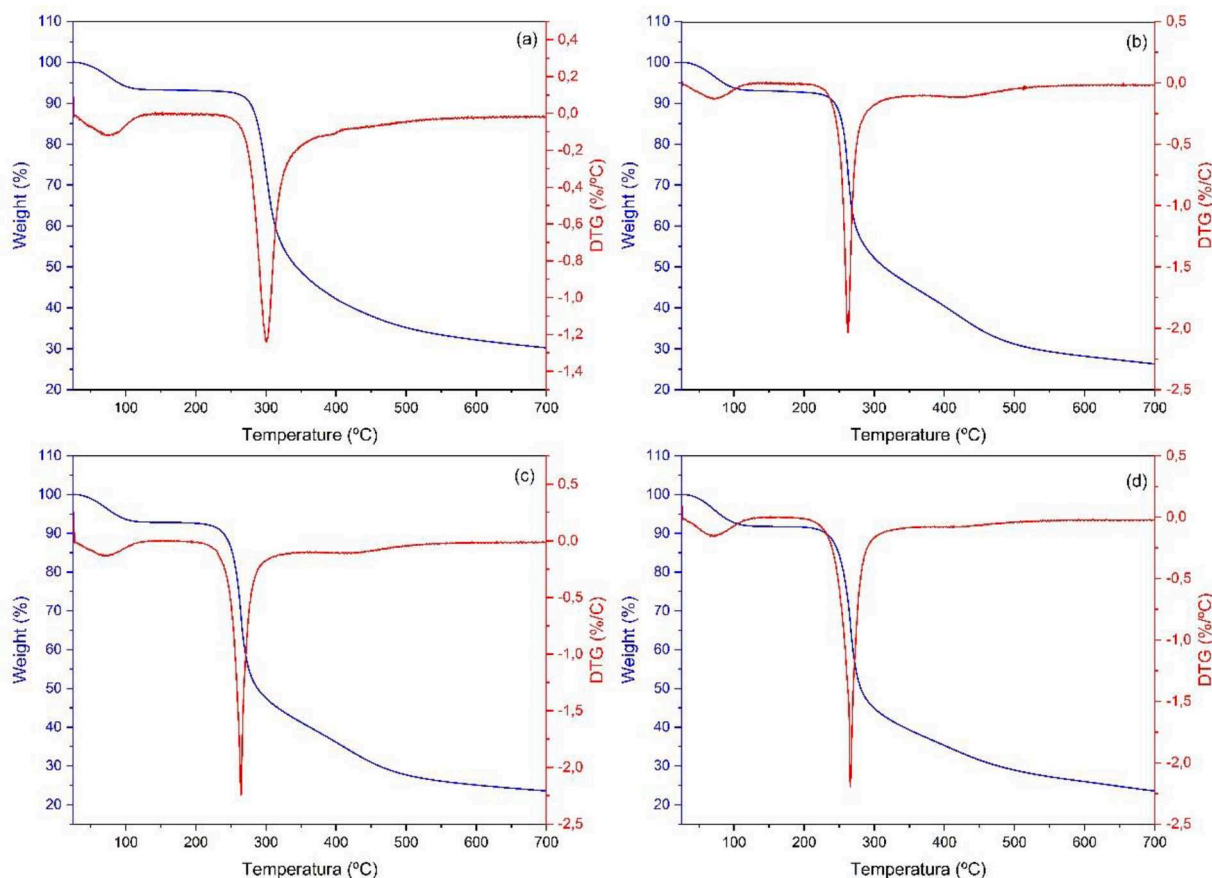


Fig. 3. TG and DTG curves obtained in the temperature range from 25 °C to 700 °C, a heating rate of 10 °C/min and under N<sub>2</sub> atmosphere (50 mL/min) for thermal decomposition of: (a) chitosan, (b) HTCC\_3, (c) HTCC\_5 and (d) HTCC\_9.

The thermogram from Fig. 3 (upper left) shows that unmodified chitosan has two notable weight loss steps upon heating. The first was between 50 and 100–110 °C, where the water desorption from the samples caused a decrease of approximately 7–8% of its original weight. The step between 270–320 °C is related to the degradation of the biopolymer and vaporization of volatile compounds. Although the maximum rate is at 300 °C, as shown by DTG curve, chitosan maintains the weight loss process until reaching 70% weight loss at 700 °C (Neto et al., 2005). (Moussout et al., 2016) also describe a third step in chitosan degradation assigned to the carbonization of residual carbon and pyranose ring from 300–500 °C, though this step is a lot smoother in this work and not easily identifiable.

All HTCC samples showed the same thermal behavior despite the difference in DS. These samples had a weight loss relative to water desorption that was similar to the unmodified sample. Water content did not alter after modification as dipole–dipole interaction between water molecules and amine or hydroxyl groups are present in all samples (De Britto & Campana-Filho, 2004). However, the temperature of the second step was reduced from 300 °C to approximately 260 °C (peak of DTG curves), occurring in the interval of 250–290 °C, close to what was reported by Hu et al. (2016). According to De Brito and Campana et al. (2004), the modification reduced the thermal stability of chitosan because quaternary functional groups weaken the hydrogen molecular interaction along the polymeric chain. The decrease in stability is also indicated by the fact that the modified samples lost nearly 75% of their initial weight at 700 °C, which is 5% more than chitosan. Although it was seen as a slight disturbance in DTG curve (at 420 °C), the third step is more noticeable for the HTCC samples.

The greater the degree of HTCC substitution, the greater the solubility of the sample (Table 1). This is due to the higher concentration of quaternary terminals that were incorporated into the amino terminals of chitosan, present in greater amounts in the samples with higher DS. The strong intra and intermolecular hydrogen bonds generate a highly ordered arrangement in chitosan, which leads to low solubility in aqueous media. The insertion of quaternary ammonium groups in its structure causes a distortion in this arrangement, decreasing the amount of these bonds and favoring solubility in water (Chen et al., 2016).

### 3.2. Effectiveness and characterization of coatings

#### 3.2.1. Structural and morphological characterization of coatings

In both PP and cotton fabrics spectra, seen in Fig. 4a, the first

apparent peak appears at 1600–1700 nm, corresponding to the axial deformation of the C=O bond from HTCC (Gavalayan, 2016). A peak at approximately 3200–3600 nm, is assigned to the axial deformation (or stretching) of the O–H bond and the N–H bond, from HTCC, indicating a successful coating process (Zhao et al., 2014). Since cellulose/cotton also contains O–H bonds, this peak is also present in the uncoated sample, as observed in the spectra of Fig. 4b. The same occurs for the peak at approximately 1656 cm<sup>-1</sup>, assigned to C–O bonds in cotton and an intense peak observed near 1030 cm<sup>-1</sup> assigned to the vibrations of the C–O and O–H bonds that correspond to the cellulosic polysaccharide (Rosa et al., 2008). After the deposition of HTCC onto the fabrics, such peaks become more intense.

The SEM micrographs of the polypropylene and cotton samples, as well as the coatings are shown in Fig. 5. According to the micrographs, it is possible to observe that there is no visible change in the morphology of the fibers between the pure tissues and the coated tissues. Furthermore, when producing thin films containing HTCC on fabrics, an increase in the diameter of the original fibers is observed as the concentration of incorporated HTCC is higher.

### 3.3. Antiviral activity and cytotoxicity assay

According to the results presented in Table 2, fabrics that were uncoated or coated with unmodified chitosan did not exhibit virucidal activity greater than 90%, even after 24 h of contact with the virus. In contrast, fabrics that were coated with HTCC achieved at least 99.9% of viral inactivation in just 1 h of contact between the virus and the samples. It is important to note that this percentage of inactivation was observed regardless of the fabric material (PP or cotton), the degree of substitution HTCC, and concentration of the HTCC solution used in the coating. Therefore, the results suggest that HTCC coating could be a promising strategy to confer antiviral properties to fabrics, regardless of their intrinsic characteristics. Milewska et al. (2016) reported that quaternary chitosan derivative interacts with the ectodomain of the S protein present in the viruses of the family *Coronaviridae*, which was also observed in SARS-CoV-2 by the same research group (Milewska et al., 2021). Inhibition occurs due to electrostatic interactions between HTCC and the S protein of coronaviruses. The authors theorize that although the interaction between a single HTCC active site and a protein site is weak, the charge distribution along the polymer causes the material to selectively interact with the viral ectodomain, inhibiting its binding with cell receptors. None of the tissue samples coated with HTCC showed a

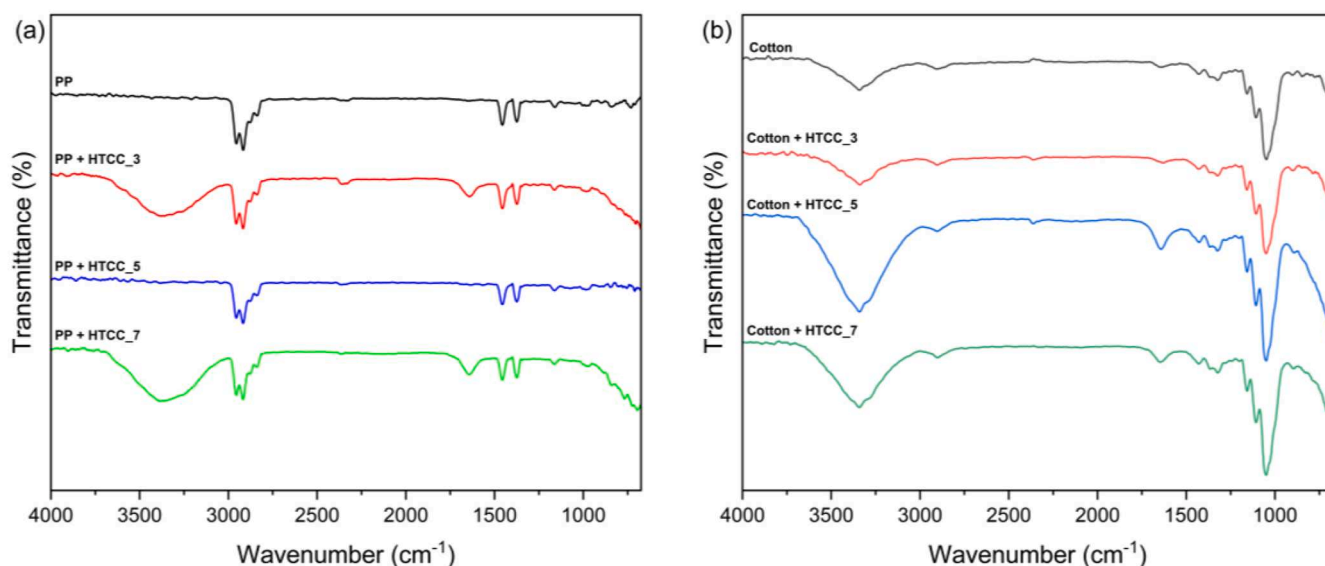


Fig. 4. ATR-FTIR spectra of polypropylene and polypropylene+HTCC samples (a); cotton and cotton+HTCC samples (b).

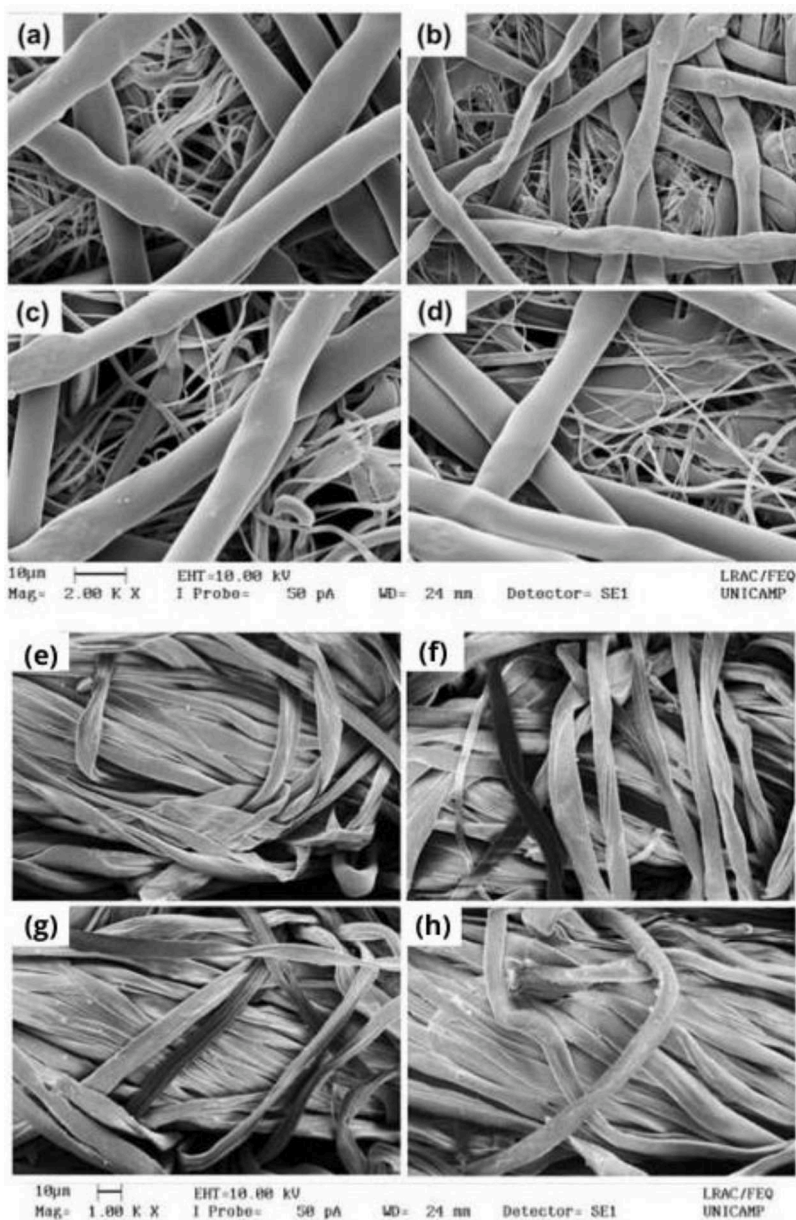


Fig. 5. SEM micrographs of (a) PP, (b) PP + HTCC\_3, (c) PP + HTCC\_5, (d) PP + HTCC\_7 samples, (e) cotton, (f) cotton + HTCC\_3, (g) cotton + HTCC\_5 and (h) cotton + HTCC\_7 samples.

**Table 2**  
Virucidal and cytotoxicity assays of uncoated and coated samples.

Sample	C <sub>HTCC</sub> (g/dL)	Time (min)	Viral Inactivation	Toxic?
PP	–	1440	<90%	Nontoxic
Cotton	–	1440	<90%	Nontoxic
PP+chitosan	1 & 0.1	1440	<90%	Nontoxic
Cotton+chitosan	1 & 0.1	1440	<90%	Nontoxic
PP+HTCC_3	1	1	99,99%	Nontoxic
	0.1	1	99,9%	
Cotton+HTCC_3	1	1	99,99%	Nontoxic
	0.1	1	99,99%	
PP+HTCC_5	1	1	99,99%	Nontoxic
	0.1	1	99,99%	
Cotton+HTCC_5	1	1	99,9%	Nontoxic
	0.1	1	99,99%	
PP+HTCC_7	1	1	99,9%	Nontoxic
	0.1	1	99,9%	
Cotton+HTCC_7	1	1	99,9%	Nontoxic
	0.1	1	99,99%	

cytotoxic effect against the cell line studied. These results are consistent with studies in the literature: Milewska et al. (2021) also evaluated the antiviral potential of HTCC and did not find cytotoxicity in contact with Vero and Vero E6 lineage cells. Wang et al., (2011) evaluated the effects of HTCC in vivo and found no toxicity of the compound during 30 days of addition to the diet of rats. Zhou et al. (2013) also did not find any cytotoxicity of the material when in contact with mouse fibroblasts.

Regardless of fabric material, degree of substitution or concentration of HTCC, all samples inactivated 99.9% of the coronavirus after 1 h of contact, which demonstrates its effectiveness in the future application as a sustainable virucidal coating for masks and respirators. Since all evaluated conditions produce effective and easily processable material, it is possible to choose an ideal coating method based on the costs of reagents. In this work, GTMAC was the most onerous reagent.

### 3.4. Antibacterial activity

#### 3.4.1. Minimum inhibitory concentration (MIC)

In the turbidity and resazurin methods applied to HTCC samples in contact with Gram-positive and Gram-negative bacteria, an increase in the DS from 59% (HTCC\_3) to 79% (HTCC\_5) causes a significant reduction in MIC, of 2 to 8 times, as shown in Table 3. However, an increase in the DS from 79% to 93% does not affect MIC for both *E. coli* and *S. aureus*, demonstrating similar behavior for gram-positive and gram-negative bacteria. The increase in the concentration of quaternary ammonium groups enhanced activity against these bacteria, up until DS of 79%. Beyond this value, little difference is noticed.

The minimum bactericidal concentration (MBC) method differs from turbidity and developer methods since the solutions containing bacteria are removed after contact with the HTCC samples and then incubated. Thus, it is possible to verify if the material caused bacteria inhibition or inactivation, since the bacterial solution is incubated without the presence of the bactericidal material, and the strains may grow. *S. aureus*, the optimized MBC presented was observed with the HTCC sample DS of 93%. For *E. coli*, the same phenomenon was observed for the other methods, where an increase in bactericidal activity was observed up until DS of 79%. Such results indicate that the material not only inhibits bacterial growth but also causes bacteria death since there was no formation of new bacteria colonies. The bactericidal activity of the HTCC is due to the ammonium functional groups present in the HTCC structure, which conferred to it a permanent positive charge capable of interacting with the negatively charged structures on the bacterial cell surface (Yang et al., 2020).

#### 3.5. Agar diffusion test and colony count test

The HTCC deposited on the fabrics did not show significant diffusion of HTCC to the medium (Table 4), as the samples were inefficient in the inactivation of bacteria in the agar diffusion test. Only the control, ampicillin, presented antibacterial activity. This result is expected since for the material to show inhibition halos, the bactericidal/inhibitory substance must diffuse from the material to the medium. It is then confirmed that there is no significant release of the active substance into the medium. For this material, it is desired that bacteria are inhibited/eliminated through direct contact with tissues containing the active substance without the release of bactericidal material. Colony count tests indicated that the coated samples were able to inactivate/eliminate bacteria via contact-killing. The samples produced by coating with solutions of 1.0 g/dL of HTCC have a greater ability to inhibit the growth of tested bacteria in both PP and cotton fabrics. Moreover, the PP+HTCC\_5\_1.0 sample was able to reduce the number of visible colonies to zero for 1D and 2D condition, proving to be highly efficient against Gram-negative and Gram-positive bacteria.

Because the bacterial cell wall is negatively charged, cationic polymers can interact and disrupt such structure. However, in this work, the HTCC also presented antibacterial activity against Gram-positive bacteria, which was also observed by other works, as reported by Hoque et al. (2016). According to these authors, HTCC causes the dissipation of the bacterial membrane potential, the leakage of  $K^+$  ions (essential for cell survival) and the possibility of permeating the cytoplasmic

**Table 3**  
Minimum inhibitory concentration of HTCC against *S. aureus* and *E. coli*.

Sample	<i>S. aureus</i> Minimum Inhibitory Concentration (µg/mL)			<i>E. coli</i>		
	Turbidity	Resazurin	MBC	Turbidity	Resazurin	MBC
HTCC_3	312.50	625.00	312.50	156.250	156.250	156.250
HTCC_5	156.25	78.12	312.50	156.25	78.12	78.12
HTCC_7	156.25	78.12	156.25	156.25	78.12	78.12
Ampicillin	0.19	0.19	0.19	0.39	0.39	0.39

**Table 4**  
Colony count test for *S. aureus* and *E. coli* bacteria after contact with HTCC-coated tissues.

Colony Count (UFC/mL)	<i>S. aureus</i>			<i>E. coli</i>		
	1D	2D	3D	1D	2D	3D
T0	149*	167	154	362	387	373
PP	227	176	206	63	61	33
Cotton	191	185	202	74	84	52
PP+HTCC_5_0.1	113	108	102	27	21	26
PP+HTCC_5_1.0	0	0	1	0	0	0
Cotton+HTCC_5_0.1	11	3*	12	34	47	20
Cotton+HTCC_5_1.0	5	6	0	20*	51*	*

Note: 3D: 3rd dilution; T0 = control, without bactericidal sample.

\* Small cluster.

membrane, leading to cell death. It can be seen in Fig. 6 how bacterial growth is inhibited when there is HTCC on cotton fabrics (Fig. 6b) and that the inhibition is even greater with tissues coated with solutions of 1 g/dL of HTCC (Fig. 6c).

### 4. Conclusion

The results of the study demonstrate that HTCC-coated cotton or polypropylene materials with degrees of substitution ranging from 59 to 93% exhibit significant antiviral activity against coronavirus and also

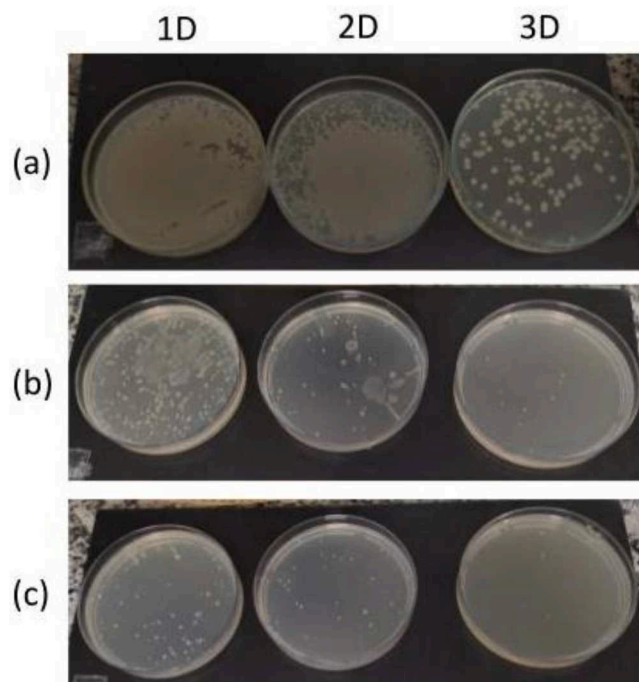


**Fig. 6.** Bacterial growth for 1 dilution (1D), 2 dilutions (2D) and 3 dilutions (3D) after incubation of *S. Aureus* with pure cotton samples (a), cotton + HTCC\_5 - 0.1 g/dL (b) and cotton + HTCC\_5 - 1.0 g/dL.

antibacterial activity against both Gram-negative and Gram-positive bacteria. This suggests that the HTCC-coated materials could be used as a safer alternative to coatings that contain hazardous chemicals or metals, with potential applications in environments where the control of infectious diseases is important. Importantly, the deposition of HTCC did not compromise the morphology of the cotton or polypropylene samples, indicating that there was no significant reduction in filtration capacity. The findings of the study suggest that the use of HTCC as a coating could provide an effective and practical method for producing materials with antimicrobial activity, which could be used in a variety of settings to prevent the spread of infectious diseases. Given the ongoing global pandemic and thinking about new pandemics, these materials could be useful to develop quicker and more efficient solutions in the future.

## Declaration of Competing Interest

The authors declare no conflict of interest.

## Data availability

Data will be made available on request.

## Acknowledgments

The authors thank the financial support of the funding agencies Coordenação de Aperfeiçoamento de Pessoal de Nível Superior (CAPES), grant number 88881.505221/2020-01 and Conselho Nacional de Desenvolvimento Científico e Tecnológico (CNPq) process no. 142649/2019-8.

## References

- Asselt, A.J., & Giffel, M.C. (2005). Pathogen resistance to sanitisers. *Handbook of Hygiene Control in the Food Industry*, 69–92. <https://doi.org/https://doi.org/10.1533/9781845690533.1.69>.
- Chen, Y., Li, J., Li, Q., Shen, Y., Ge, Z., Zhang, W., & Chen, S. (2016). Enhanced water-solubility, antibacterial activity and biocompatibility upon introducing sulfobetaine and quaternary ammonium to chitosan. *Carbohydrate Polymers*, 143, 246–253. <https://doi.org/10.1016/j.carbpol.2016.01.073>.
- Cho, J., Grant, J., Piquette-Miller, M., & Allen, C. (2006). Synthesis and physicochemical and dynamic mechanical properties of a water-soluble chitosan derivative as a biomaterial. *Biomacromolecules*, 7(10), 2845–2855. <https://doi.org/10.1021/bm060436s>.
- Das, S., Samanta, S., Banerjee, J., Pal, A., Giri, B., Kar, S. S., & Dash, S. K. (2022). Is Omicron the end of pandemic or start of a new innings? *In Travel Medicine and Infectious Disease* (Vol. 48). <https://doi.org/10.1016/j.tmaid.2022.102332>
- De-Britto, D., & Campana-Filho, S. P. (2004). A kinetic study on the thermal degradation of N,N,N-trimethylchitosan. *Polymer Degradation and Stability*, 84(2), 353–361. <https://doi.org/10.1016/j.polyimdegstab.2004.02.005>
- Domard, A., Rinaudo, M., & Terrassin, C. (1986). *New method for the quaternization of chitosan*. [https://doi.org/10.1016/0141-8130\(86\)90007-3](https://doi.org/10.1016/0141-8130(86)90007-3).
- Freitas, E. D., Moura, C. F., Kerwald, Jr., & Beppu, M. M. (2020). An Overview of Current Knowledge on the Properties, Synthesis and Applications of Quaternary Chitosan Derivatives. *Polymers*, 12(12), 2878. <https://doi.org/10.3390/polym12122878>
- Gavalyan, V.B. (2016). Synthesis and characterization of new chitosan-based Schiff base compounds. *Carbohydrate Polymers*, 145, 37–47. <https://doi.org/10.1016/j.carbpol.2016.02.076>.
- Gralinski, L. E., & Menachery, V. D. (2020). Return of the coronavirus: 2019-nCoV. *In Viruses*, 12(2). <https://doi.org/10.3390/v12020135>
- Hoffmann, M., Krüger, N., Schulz, S., Cossmann, A., Rocha, C., Kempf, A., Nehlmeier, I., Graichen, L., Moldenhauer, A. S., Winkler, M. S., Lier, M., Dopfer-Jablonka, A., Jäck, H. M., Behrens, G. M. N., & Pöhlmann, S. (2022). The Omicron variant is highly resistant against antibody-mediated neutralization: Implications for control of the COVID-19 pandemic. *Cell*, 185(3), 447–456. <https://doi.org/10.1016/j.cell.2021.12.032>. e11.
- Hoque, J., Adhikary, U., Yadav, V., Samaddar, S., Konai, M. M., Prakash, R. G., Paramanandham, K., Shome, B. R., Sanyal, K., & Halder, J. (2016). Chitosan Derivatives Active against Multidrug-Resistant Bacteria and Pathogenic Fungi. *In Vivo Evaluation as Topical Antimicrobials*. *Molecular Pharmaceutics*, 13(10), 3578–3589. <https://doi.org/10.1021/acs.molpharmaceut.6b00764>
- Hu, D., Wang, H., & Wang, L. (2016). Physical properties and antibacterial activity of quaternized chitosan/carboxymethyl cellulose blend films. *LWT*, 65, 398–405. <https://doi.org/10.1016/j.lwt.2015.08.033>
- Huang, J., Cheng, Z. H., Xie, H. H., Gong, J. Y., Lou, J., Ge, Q., Wang, Y. J., Wu, Y. F., Liu, S. W., Sun, P. L., & Mao, J. W. (2014). Effect of quaternization degree on physicochemical and biological activities of chitosan from squid pens. *International Journal of Biological Macromolecules*, 70, 545–550. <https://doi.org/10.1016/j.ijbiomac.2014.07.017>
- Kampf, G., Brüggemann, Y., Kaba, H. E. J., Steinmann, J., Pfaender, S., Scheithauer, S., & Steinmann, E. (2020). Potential sources, modes of transmission and effectiveness of prevention measures against SARS-CoV-2. *Journal of Hospital Infection*, 106(4), 678–697. <https://doi.org/10.1016/j.jhin.2020.09.022>
- Katikireddi, S. V., Cerqueira-Silva, T., Vasileiou, E., Robertson, C., Amele, S., Pan, J., Taylor, B., Boaventura, V., Werneck, G. L., Flores-Ortiz, R., Agrawal, U., Docherty, A. B., McCowan, C., McMenamin, J., Moore, E., Ritchie, L. D., Rudan, I., Shah, S. A., Shi, T., & Sheikh, A. (2022). Two-dose ChAdOx1 nCoV-19 vaccine protection against COVID-19 hospital admissions and deaths over time: a retrospective, population-based cohort study in Scotland and Brazil. *The Lancet*, 399, 25–35. [https://doi.org/10.1016/S0140-6736\(21\)02754-9](https://doi.org/10.1016/S0140-6736(21)02754-9), 10319.
- Li, Z., Yang, F., & Yang, R. (2015). Synthesis and characterization of chitosan derivatives with dual-antibacterial functional groups. *International Journal of Biological Macromolecules*, 75, 378–387. <https://doi.org/10.1016/j.ijbiomac.2015.01.056>
- Mathieu, E., Ritchie, H., Ortiz-Ospina, E., Roser, M., Hasell, J., Appel, C., Giattino, C., & Rodés-Guirao, L. (2021). A global database of COVID-19 vaccinations. *Nature Human Behaviour*, 5(7), 947–953. <https://doi.org/10.1038/s41562-021-01122-8>
- Milewska, A., Chi, Y., Szczepanski, A., Barreto-Duran, E., Dabrowska, A., Botwina, P., Obloza, M., Liu, K., Liu, D., Guo, X., Ge, Y., Li, J., Cui, L., Ochman, M., Urlik, M., Rodziejewicz-Motowidlo, S., Zhu, F., Szczubialka, K., Nowakowska, M., & Pyrc, K. (2021). HTCC as a Polymeric Inhibitor of SARS-CoV-2 and MERS-CoV. *Journal of Virology*, (4), 95. <https://doi.org/10.1128/jvi.01622-20>
- Milewska, A., Ciejka, J., Kaminski, K., Karewicz, A., Bielska, D., Zeglen, S., Karolak, W., Nowakowska, M., Potempa, J., Bosch, B. J., Pyrc, K., & Szczubialka, K. (2013). Novel polymeric inhibitors of HCoV-NL63. *Antiviral Research*, 97(2), 112–121. <https://doi.org/10.1016/j.antiviral.2012.11.006>
- Milewska, A., Kaminski, K., Ciejka, J., Kosowicz, K., Zeglen, S., Wojarski, J., Nowakowska, M., Szczubialka, K., & Pyrc, K. (2016). HTCC: Broad range inhibitor of coronavirus entry. *PLoS ONE*, (6), 11. <https://doi.org/10.1371/journal.pone.0156552>
- Moussouh, H., Ahlafi, H., Aazza, M., & Bourakhouadar, M. (2016). Kinetics and mechanism of the thermal degradation of biopolymers chitin and chitosan using thermogravimetric analysis. *Polymer Degradation and Stability*, 130, 1–9. <https://doi.org/10.1016/j.polyimdegstab.2016.05.016>
- Neto, C. G. T., Giacometti, J. A., Job, A. E., Ferreira, F. C., Fonseca, J. L. C., & Pereira, M. R. (2005). Thermal analysis of chitosan based networks. *Carbohydrate Polymers*, 62(2), 97–103. <https://doi.org/10.1016/j.carbpol.2005.02.022>
- Qin, Y., Li, P., & Guo, Z. (2020). Cationic chitosan derivatives as potential antifungals: A review of structural optimization and applications. *Carbohydrate Polymers*, 236, Article 116002. <https://doi.org/10.1016/j.carbpol.2020.116002>. November 2019.
- Ramakrishnan, M. A. (2016). Determination of 50% endpoint titer using a simple formula. *World Journal of Virology*, 5(2), 85. <https://doi.org/10.5501/wjv.v5.i2.85>
- Roque-Borda, C. A., Antunes, B. F., Toledo-Borges, A. B., Costa-De-Pontes, J. T., Meneguín, A. B., Chorilli, M., Trovatti, E., Teixeira, S. R., Pavan, F. R., & Vicente, E. F. (2022). Conjugation of Ctx(Ile21)-Ha Antimicrobial Peptides to Chitosan Ultrathin Films by N-Acetylcysteine Improves Peptide Physicochemical Properties and Enhances Biological Activity. *ACS Omega*, 7(32), 28238–28247. <https://doi.org/10.1021/acsomega.2c02570>
- Roque-Borda, C. A., Saraiva, M., de, M. S., Macedo Junior, W. D., Márquez Montesinos, J. C. E., Meneguín, A. B., Toledo-Borges, A. B., Crusca Junior, E., Garrido, S. S., de Almeida, A. M., Marchetto, R., Chorilli, M., Berchieri Junior, A., Teixeira, S. R., Pavan, F. R., & Vicente, E. F. (2023). Chitosan and HPMCA double-coating as protective systems for alginate microparticles loaded with Ctx(Ile21)-Ha antimicrobial peptide to prevent intestinal infections. *Biomaterials*, 293. <https://doi.org/10.1016/j.biomaterials.2022.121978>
- Rosa, S., Laranjeira, M. C. M., Riehl, H. G., & Fávère, V. T. (2008). Cross-linked quaternary chitosan as an adsorbent for the removal of the reactive dye from aqueous solutions. *Journal of Hazardous Materials*, 155(1–2), 253–260. <https://doi.org/10.1016/j.jhazmat.2007.11.059>
- Spinelli, V.A., Laranjeira, M.C.M., & Fávère, V.T. (2004). Preparation and characterization of quaternary chitosan salt: Adsorption equilibrium of chromium (VI) ion. *Reactive and Functional Polymers*, 61(3), 347–352. <https://doi.org/10.1016/j.reactfunctpolym.2004.06.010>
- Wang, L., Qin, C., Wang, W., & Li, W. (2011). Effect of orally administered N-(2-hydroxy) propyl-3-trimethyl ammonium chitosan on the levels of iron, zinc, copper, calcium and lead in mice. *Carbohydrate Polymers*, 84(4), 1289–1292. <https://doi.org/10.1016/j.carbpol.2011.01.025>
- Wang, W., Meng, Q., Li, Q., Liu, J., Zhou, M., Jin, Z., & Zhao, K. (2020). Chitosan derivatives and their application in biomedicine. *In International Journal of Molecular Sciences*, 21(2). <https://doi.org/10.3390/ijms21020487>
- Yang, Y., Xing, R., Liu, S., Qin, Y., Li, K., Yu, H., & Li, P. (2020). Chitosan, hydroxypropyltrimethyl ammonium chloride chitosan and sulfated chitosan nanoparticles as adjuvants for inactivated Newcastle disease vaccine. *Carbohydrate Polymers*, 229. <https://doi.org/10.1016/j.carbpol.2019.115423>
- Zhao, J., Li, J., Jiang, Z., Tong, R., Duan, X., Bai, L., Shi, J., & Chitosan, N (2020). N,N-trimethyl chitosan (TMC) and 2-hydroxypropyltrimethyl ammonium chloride chitosan (HTCC): The potential immune adjuvants and nano carriers. *International*

*Journal of Biological Macromolecules*, 154, 339–348. <https://doi.org/10.1016/j.ijbiomac.2020.03.065>

Zhao, L., Hu, Y., Xu, D., & Cai, K. (2014). Surface functionalization of titanium substrates with chitosan-lauric acid conjugate to enhance osteoblasts functions and inhibit bacteria adhesion. *Colloids and Surfaces B: Biointerfaces*, 119, 115–125. <https://doi.org/10.1016/j.colsurfb.2014.05.002>

Zhou, Y., Yang, H., Liu, X., Mao, J., Gu, S., & Xu, W. (2013). Potential of quaternization-functionalized chitosan fiber for wound dressing. *International Journal of Biological Macromolecules*, 52(1), 327–332. <https://doi.org/10.1016/j.ijbiomac.2012.10.012>

## Further reading

Deng, S.-Q., & Peng, H.-J. (2020). Characteristics of and Public Health Responses to the Coronavirus Disease. 2019 Outbreak in China. *Journal of Clinical Medicine*, 9(2), 575. <https://doi.org/10.3390/jcm9020575>